Published in final edited form as:
Neuroscience. 2020 March 01; 429: 92–105. doi:10.1016/j.neuroscience.2019.12.009.

High Behavioral Sensitivity to Carbon Dioxide Associates with Enhanced Fear Memory and Altered Forebrain Neuronal Activation

Katherine M. J. McMurray[a], **Alijah Gray**[b], **Paul Horn**[c], **Renu Sah**[a,d,*]

[a]Department of Pharmacology & Systems Physiology, University of Cincinnati, United States

[b]Undergraduate Program, Dept. of Psychology, University of Cincinnati, United States

[c]Neurology Division, Children's Hospital Medical Center and College of Medicine, University of Cincinnati, United States

[d]Veterans Administration (VA) Medical Centre, Cincinnati, OH 45237, United States

Abstract

There is considerable interest in pre-trauma individual differences that may contribute to increased risk for developing post-traumatic stress disorder (PTSD). Identification of underlying vulnerability factors that predict differential responses to traumatic experiences is important. Recently, the relevance of homeostatic perturbations in shaping long-term behavior has been recognized. Sensitivity to CO_2 inhalation, a homeostatic threat to survival, was shown to associate with the later development of PTSD symptoms in veterans. Here, we investigated whether behavioral sensitivity to CO_2 associates with PTSD-relevant behaviors and alters forebrain fear circuitry in mice. Mice were exposed to 5% CO_2 or air inhalation and tested one week later on acoustic startle and footshock contextual fear conditioning, extinction and reinstatement. CO_2 inhalation evoked heterogenous freezing behaviors (high freezing CO_2-H and low freezing CO_2-L) that significantly associated with fear conditioning and extinction behaviors. CO_2-H mice elicited potentiated conditioned fear and delayed extinction while behavioral responses in CO_2-L mice were similar to the air group. Persistent neuronal activation marker ΔFosB immunostaining revealed altered regional neuronal activation within the hippocampus, amygdala and medial pre-frontal cortex that correlated with conditioned fear and extinction. Inter-regional co-activation mapping revealed disruptions in the coordinated activity of hippocampal dentate-amygdala-infralimbic regions and infralimbic-prelimbic associations in CO_2-H mice that may explain their enhanced fear phenotype. In conclusion, our data support an association of behavioral sensitivity to interoceptive threats such as CO_2 with altered fear responding to exteroceptive threats and suggest that "CO_2-sensitive" individuals may be susceptible to developing PTSD.

*Correspondence to: Renu Sah, Dept. of Pharmacology & Systems Physiology, University of Cincinnati, UC North Reading Campus, 2170 East Galbraith Road, Cincinnati, OH 45237, United States. sahr@uc.edu (R. Sah).

CONFLICT OF INTEREST
The authors declare no conflict of interest

Keywords

CO_2 sensitivity; PTSD; fear; startle; extinction

INTRODUCTION

Effective regulation of fear is essential for optimal mental health. Failure to regulate fear is a hallmark of many psychiatric conditions, particularly post-traumatic stress disorder (PTSD), a highly debilitating condition afflicting ~8% of the general population and ~22% of combat veterans annually (Kessler et al., 1995; Thomas et al., 2010). Most trauma-exposed individuals experience transient after-effects that resolve within one month. However, in about 10–20% of cases, symptoms persist, resulting in PTSD (Ross et al., 2017). There is considerable interest in the identification of pre-trauma factors that associate with and can predict differential fear responses and vulnerability to PTSD.

Mounting evidence supports a primary role of interoception described as an individual's sensing and subjective awareness of the "physiological condition of the body itself" in the regulation of emotional responses (Craig, 2002; 2003). Maintaining homeostasis is critical for an organism's survival, and interoception is a powerful driver of behaviors directed toward this goal (Khalsa et al., 2018). Individuals with PTSD have increased interoceptive sensitivity (Boettcher et al., 2016), supported by increased emotional and physiological reactivity to interoceptive triggers such as sodium lactate (Muhtz et al., 2012) and carbon dioxide (CO_2) (Muhtz et al., 2011; Kellner et al., 2018) resulting in fear, panic attacks and intrusive flashbacks. However, it is not well understood whether this sensitivity to interoceptive triggers exists pre-trauma, prior to the development of PTSD. Interestingly, pre-deployment studies in veterans reported that soldiers with high emotional reactivity to CO_2 inhalation later exhibited significantly higher PTSD symptoms during deployment (Telch et al., 2012), suggesting that high CO_2 sensitivity may serve as a potential risk factor for PTSD development. The physiologic effects of CO_2, a potent interceptive stimulus, result from increased acidosis (H^+), constituting a homeostatic threat to survival. In humans, CO_2 produces heterogenous, dose-dependent responses (Colasanti et al., 2008), and individuals on the high spectrum of CO_2 sensitivity may be at risk for subsequent psychopathology (Battaglia, 2017). Collectively, these findings underscore the utility of CO_2 inhalation as a contributory factor in promoting individual differences in fear regulation relevant to PTSD and highlight the need for translational studies for understanding contributory mechanisms.

With these considerations, the current study investigated: (a) whether prior CO_2 inhalation in mice impacts delayed behavioral responses to two discrete exteroceptive experiences relevant to posttraumatic physiology, contextual fear conditioning and extinction, as well as acoustic startle reactivity, (Maren et al., 2013; Whitaker et al., 2014; Morgan et al., 2015; Liberzon and Abelson, 2016), and, (b) whether variation in CO_2 response associates with fear and startle reactivity. Recent studies have reported modulation of fear extinction in rats by carbon dioxide (CO_2) inhalation (Monfils et al., 2018), although effects on other PTSD relevant behaviors or fear regulatory circuits was not investigated. We also hypothesized an association of CO_2 sensitivity with altered neuronal activation within primary fear regulatory

amygdala–prefrontal–hippocampal areas that are implicated in PTSD (Etkin and Wager, 2007; Koenigs et al., 2008; Michopoulos et al., 2017). Our data revealed potentiated fear conditioning and delayed extinction in "CO_2-sensitive" mice as well as perturbations in dentate–cortico–amygdala activation patterns.

EXPERIMENTAL PROCEDURES

Animals

Studies were performed using adult male BALB/c mice ($N = 40$, Envigo, Indianapolis, IN; similar numbers have been used for this strain in previous studies for investigation of within-strain behavioral effects (Loos et al., 2015). This strain has been used in previous CO_2-evoked behavior studies by our group (Vollmer et al., 2016; McMurray et al., 2019). Mice were pair housed in a climate-controlled vivarium (temperature 23 ± 4 C, humidity 30 ± 6%) on a 14 h/10 h light/dark cycle. All study protocols were approved by the Institutional Animal Care and Use Committee of the University of Cincinnati and performed in a vivarium accredited by the Association for Assessment and Accreditation of Laboratory Animal Care.

Behavioral manipulations

To investigate whether an aversive interoceptive experience can regulate delayed responses to exteroceptive triggers, mice were exposed to CO_2 inhalation and subjected to acoustic startle and footshock contextual fear conditioning after one week (see Fig. 1 for experimental layout). The rationale for the one week delay was for temporal consistency with other paradigms assessing PTSD-relevant behaviors after a 7 d period following experimental manipulations (McGuire et al., 2010; Lisieski et al., 2018) and to avoid any acute effects of CO_2 inhalation given observation of conditioned fear behavior the day after inhalation (Vollmer et al., 2016; McMurray et al., 2019).

CO_2-inhalation paradigm

Mice were subjected to air or CO_2 inhalation as described in previous studies by our group and others (Ziemann et al., 2009; Taugher et al., 2014; Vollmer et al., 2016; McMurray et al., 2019; Winter et al., 2019) using a dual vertical Plexiglas chamber (25.5 cm × 29 cm × 28 cm per chamber). Air or 5% CO_2 (in 21% O_2, balanced with N_2, Wright Brothers Inc., Cincinnati, OH) was infused in the upper chamber while the mice were placed in the lower compartment to avoid direct blowing of the gas which is highly aversive to rodents. A flow meter with a steady infusion rate of 10 L/min was used for all animals and the concentration of CO_2 within the lower chamber was verified (5.0 ± 0.5%) by the CARBOCAP® GM70 carbon dioxide meter (GMP221 probe with accuracy specification +/− 0.5%) (Vaisala, Helsinki, Finland).

Mice were habituated to a CO_2 chamber (Day 1). The following day, mice were returned to the chamber and exposed to air or 5% CO_2 for 10 min during which time freezing behavior was assessed. The day after CO_2 exposure animals were returned to the chamber for 5 min in the absence of CO_2. The contextual exposure is important for supporting CO_2 inhalation freezing as a fear-associated behavioral response. Mice were video recorded for

later analysis. Freezing (complete lack of movement except for respiration) was scored using automated FreezeScan software (CleverSys Inc.).

Acoustic Startle

One week following the CO_2 exposure, startle response to an unexpected acoustic stimulus was measured using the SR-LAB startle response system (San Diego Instruments, San Diego, CA) as previously described with modifications (Schmeltzer et al, 2015). The enclosure was of sufficient size to restrict but not restrain the animal and allowed it to turn around. The chambers were calibrated using the SR-LAB standardization unit (San Diego Instruments, San Diego, CA), prior to testing. Background noise in the chamber was maintained at 68 dB. After a 5-min acclimatization period, mice were exposed to 10 trials of 110 dB stimuli over the 68-dB background (40 ms duration; 30–38 s inter-trial interval) followed by 30 trials included randomly generated 0, 95, 100, 110, 115 and 120db stimuli over background (40 ms duration; 30–38 s inter-trial interval). Movement inside the tube was detected by a piezoelectric accelerometer below the frame. For each trial, measurements were taken at 1 ms intervals for a response window of 150 ms following the startle stimulus using National Instruments Data Acquisition Software (San Diego Instruments, San Diego, CA). The maximum response amplitude (Vmax; mV) within the recording window was used for data.

Contextual fear conditioning

Mice underwent a footshock contextual conditioning paradigm to investigate fear acquisition, conditioned fear, extinction and reinstatement following previously published procedures from our group (Vollmer et al., 2013; Schubert et al., 2018) with modifications. Operant chambers housed in sound attenuated isolation cabinets were used (Clever Sys Inc.). The floors of the chambers consisted of stainless steel grid bars that delivered scrambled electric shocks. The grid, floor trays and chamber walls were wiped with 10% ethanol and allowed to dry completely. Mice were allowed to acclimate for 5 min before receiving three shocks (0.5 mA, 1 s duration, 1 min apart). The animals were returned to the chamber the next 6 days and behaviors were recorded for 5 min without shocks to measure conditioned fear and extinction. Following the last extinction trial, mice received one shock (0.5 mA, 1 s) and remained in the chamber for 5 min to measure reinstatement of fear. Freezing was scored using automated FreezeScan software (CleverSys Inc.).

Immunohistochemistry (IHC)

The day after reinstatement of fear, mice were perfused transcardially with 4% paraformaldehyde and processed for IHC as previously described (Vollmer et al., 2016; McMurray et al., 2019). Briefly, 30 μm coronal brain sections were cut and stored in cryoprotectant (0.1 M phosphate buffer, 30% sucrose, 1% polyvinylpyrrolidone, and 30% ethylene glycol) at −20 °C until immunolabeled using primary anti-bodies against FosB (Rb anti-FosB 1:5000 in blocking buffer; Santa Cruz Biotechnologies, sc-7203). The following day, sections were washed again five times for 5 min in PBS, then incubated in biotinylated secondary antibody, (Biotinylated Goat anti-Rb 1:400 in blocking solution; Vector Labotatories, BA-1000) for 1 h. Sections were washed again five times for 5 min each in PBS, and were then incubated in avidin-biotin complex using ABC Vectastain kit,

diluted 1:800 for 1 h. Following washes, sections were incubated in diaminobenzadine (DAB, Pierce, Rockford, IL) and H_2O_2 for approximately 10 min. To maintain consistency between samples, all sections were processed for immunostaining in the same run at the same time. Subsequently, sections were mounted onto Gold Seal UltraStick microscope slides followed by dehydration in Xylene solutions. Finally, slides were cover-slipped using DPX (Sigma, 44581).

Image analysis and cell counting

Immunolabeled sections were mounted and imaged at 5× using an AxioImager ZI microscope (Axiocam MRm camera and AxioVision Release 4.6 software; Zeiss). Immunopositive areas were selected for analysis based on their role in regulation of defensive behaviors and CO_2 chemosensory mechanisms. Regions were selected for full quantification and analysis if preliminary assessments of ΔFosB expression suggested differences between experimental groups. These areas included the dorsal and ventral dentate gyri of the hippocampus (dDG, AP −1.34 to −2.92; and vDG, AP −2.92 to −3.60), the medial prefrontal cortex (mPFC) including both the infralimbic (IL, AP 1.98–1.34) and prelimbic (PL, AP 1.98–1.42) cortices, basolateral (BLA, AP −0.94 to −2.06) and central (CeA, AP −0.94 to −2.06) nuclei of the amygdala, bed nucleus of stria terminalis (BNST, AP 0.68–0.14) and the nucleus accumbens (NAc, AP 1.42–0.74). Brain areas not included in the analysis had negligible FosB immunopositive cells. Regions were delineated using characteristics of each nucleus based on the atlas of Paxinos and Watson (1998). At least 3–4 images per region of interest per hemisphere were collected for each mouse. ΔFosB immune-positive cells were counted using the Image-J “cell counter” tool (ImageJ, NIH) by an investigator blind to experimental group. Cell counts for each section were averaged for each animal and individual means averaged to derive group means.

Brain functional activity-connectivity analysis

For functional connectivity mapping, pairwise Pearson correlation coefficients were determined for interregional ΔFosB signals in all groups (e.g., air, CO_2-low (CO_2-L), CO_2-high (CO_2-H)), as described by us recently (McMurray et al., 2019) with modifications. To evaluate interregional correlations across conditions, correlation matrices were generated and plotted as heatmaps (using SAS ® version 9.4). Then, functional networks were constructed for all interregional correlations >0.5 as previously described (Moreno-Fernández et al., 2017) with modifications.

Statistical analysis

Data are represented as means ± standard error and inferential statistical analyses included one-way analyzed by analysis of variance (ANOVA), two-way repeated measures ANOVA (with adjusted degrees of freedom for the denominators) or Students’ unpaired t-test as appropriate. For *post hoc* analyses, Tukey’s Multiple Comparison tests or Bonferroni (following two-way repeated measures) were applied. Non-parametric tests were applied to distributions failing normality as determined by the Kolmogorov–Smirnov test. The log-rank Mantel–Cox test was used to analyze survival curves and determine differences in the percentage of mice that reached an extinction criterion set to 15% freezing. (Represents average freezing within the control group on the final two days of extinction when no further

decrement is noted.) Grubbs' tests were performed to determine and remove any outliers. Results were considered statistically significant at the $p < 0.05$ level and statistical analyses were performed in *Prism* (GraphPad Software, Inc., La Jolla, CA) and SAS ® version 9.4 (SAS Institute Inc., Cary, NC).

Experimental groups

For scientific reproducibility and rigor, data were collected from two separate cohorts of mice run in separate experiments separated by months and data were grouped for final behavioral analysis. Analysis of the behavioral data for CO_2 exposure revealed that the data were not normally distributed (Shapiro–Wilk normality test $p = 0.024$, Kolmogorov–Smirnov test $p = 0.020$), while air data elicited normal distribution ($p > 0.1$). A frequency distribution (Fig. 2C) suggested a bimodal spread with distinct groups of subjects within the population. Therefore, for analysis purposes, animals were divided into high and low freezers based on a median split of the percent freezing duration during CO_2 inhalation (Day 2). Mice with freezing values greater than the median were classified as CO_2-high freezers (CO_2-H), while mice with less than the median freezing values were classified as CO_2-low freezers (CO_2-L). A subset of animals (Cohort 2, $N = 22$) were processed for immunohistochemical analysis.

RESULTS

CO_2-inhalation evokes heterogenous fear-associated behaviors in mice

No significant differences in freezing were observed between air/CO_2 groups during habituation exposure to a novel context ($T_{36} = 1.302$, $p = 0.201$, unpaired t test) (Fig. 2A) suggesting there were no pre-existing differences between groups in this behavior. The next day, mice were exposed to air or CO_2. Since freezing in the CO_2 group showed non-normal distribution (Kolmogorov–Smirnov test $p = 0.021$) group differences were determined by non-parametric Mann–Whitney test. CO_2-exposed mice froze significantly more than air-exposed mice ($p = 0.014$, Two-Tailed Mann–Whitney $U = 96$) (Fig. 2B). Freezing in response to CO_2 was also found to be highly variable as evidenced by a high standard deviation (SD Air = 7.613, CO_2 = 17.71) and difference in variance compared with air-exposed mice (F-Test to compare variances $F(1,18) = 5.412$, $p = 0.0008$). Frequency distribution histogram (Fig. 2C) revealed subpopulations within the CO_2-exposed mice, with a group showing freezing behavior that largely overlapped with air exposed mice (CO_2-L) and the other separated by higher freezing (CO_2-H). Dichotomization into CO_2-H and CO_2-L subgroups using a median split resulted in normal data distribution and group differences were analyzed by ANOVA. As expected, no significant differences were noted during habituation (Fig. 2D). There was an overall effect of group on CO_2-evoked freezing ($F(2,37) = 39.840$, $p < 0.0001$) (Fig. 2E). Tukey's post hoc tests revealed significant differences between air and CO_2-H groups ($p < 0.0001$), as well as, CO_2-L and CO_2-H responder groups ($p < 0.0001$), but no significant differences between air and CO_2-L cohorts ($p > 0.05$). The next day (day 3), mice were re-exposed to the same context in the absence of air or CO_2 to assess conditioned fear (Fig. 2F). One-way ANOVA revealed an overall effect of group ($F(2,38) = 4.027$, $p = 0.026$). Tukey's post hoc tests revealed significant differences between

air and CO_2-H cohorts as well as CO_2-low and CO_2-high responder groups ($p < 0.05$), but no significant differences between air and CO_2-low groups ($p > 0.05$).

Acoustic Startle response in air and CO_2 mice

Air and CO_2 mice were exposed to a variable range of acoustic stimuli one week following inhalation (Fig. 3). There was a significant overall effect of decibel ($F(5,30) = 58.150$, $p < 0.0001$) on startle amplitude, but no significant overall effect of inhalation ($F(2,34) = 2.16$, $p = 0.131$) or interaction of inhalation with decibel ($F(10,43) = 1.450$, $p = 0.193$).

Exaggerated fear conditioning and delayed extinction in CO_2-high mice

Delayed effects of interoceptive threat CO_2 on fear regulation were assessed using a contextual fear conditioning/extinction/reinstatement paradigm one week after the inhalation exposure. Freezing during the habituation period prior to shocks on acquisition day was not significantly different between the groups ($F(2, 35) = 1.500$, $p > 0.05$) (Fig. 4A), suggesting that prior air/CO_2 exposure or acoustic startle testing did not impact baseline behavioral responses prior to footshocks. For fear acquisition (Fig. 4B) there was a significant effect of time ($F(3,34) = 45.67$, $p < 0.0001$). The effect of inhalation did not reach statistical significance ($F(2,36) = 3.07$, $p = 0.059$) and no interaction of time × inhalation ($F(6,43.93) = 1.56$, $p = 0.182$) was observed. No significant differences in mean freezing were observed after the final trial ($p > 0.05$) (Fig. 4B inset) suggesting similar acquisition of fear between groups.

On exposure to context 24 h later, higher freezing was observed in CO_2 exposed mice (Fig. 4C). There was a significant effect of inhalation ($F(2,36) = 3.74$, $p = 0.033$) and time ($F(4,33) = 28.83$, $p < 0.0001$), but no inhalation × time interaction $F(8,45.3) = 1.68$, $p = 0.130$). Post hoc analysis revealed significantly higher freezing in CO_2-H mice compared to air mice at 1, 2, 3 and 5 min ($p < 0.05$). No significant differences were noted between air and CO_2-L mice.

Repeated exposure to context for the next 5 days for extinction learning revealed marked differences in freezing between groups. CO_2-H mice elicited delayed extinction learning compared to air and CO_2-L groups (Fig. 4D). There was a significant overall effect of time ($F(4,33) = 8.17$, $p = 0.0001$) and a significant interaction of inhalation and time ($F(8,45.3) = 2.99$, $p = 0.009$), while the effect of inhalation approached significance ($F(2,36) = 2.99$, $p = 0.063$). Post hoc analysis revealed significantly higher freezing in CO_2-H mice compared to air and CO_2-L mice (CO_2-H vs air: extinction days 3 $p < 0.05$, 4 $p < 0.01$; CO_2-H vs CO_2-L: extinction days 2, 3 $p < 0.05$). There were no significant differences between air and CO_2-L mice on any of the extinction days. To further illustrate this delayed extinction learning in CO_2-H mice, a log-rank Mantel–Cox test was used to determine survival probabilities and evaluate whether groups differed in the number of days needed to reach an extinction criterion (set to 15% freezing). CO_2-H mice took significantly longer to reach criterion (Fig. 4E; χ^2; df = 2, $p = 0.042$).

Following their final extinction session mice received a reminder shock for reinstatement of fear (Fig. 4F). Analysis of pre and post shock freezing using repeated measures ANOVA revealed a significant effect of time ($F(1,36) = 15.06$, $p = 0.0004$), but no effect of inhalation

($F(2,36) = 2.05$, $p = 0.144$) nor time × inhalation interaction was observed ($F(2,36) = 0.49$, $p = 0.618$).

CO_2 evoked freezing associates with startle and fear conditioning

Spearman correlations were used to determine the association of freezing to air or CO_2 inhalation with subsequent startle amplitude across decibels as well as freezing during different phases of fear conditioning and extinction (Table 1). No significant correlations were observed between air-evoked freezing and startle responses, freezing during fear conditioning or extinction. On the contrary, significant correlations were observed within the CO_2 exposed group. Despite no group differences in acoustic startle behavior, CO_2 freezing showed a positive correlation with startle amplitude [100 db ($r = 0.583$, $p = 0.011$) while data did not reach significance for 110 db ($r = 0.455$, $p = 0.058$) and 120 db ($r = 0.408$, $p = 0.093$)]. Freezing during CO_2 also showed significant positive correlation with freezing during extinction phase of the fear conditioning paradigm, specifically extinction days 2 ($r = 0.551$, $p = 0.015$) and 3 ($r = 0.514$, $p = 0.024$) and a positive association which did not reach significance on extinction day 4 ($r = 0.416$, $p = 0.077$). Interestingly, CO_2 freezing also showed a positive correlation with pre-shock freezing ($r = 0.606$, $p = 0.006$).

CO_2-inhalation alters neuronal activation in forebrain circuitry regulating defensive behaviors

Significant changes in ΔFosB immunopositive ($\Delta FosB^+$) cell counts were observed in several areas (Fig. 5). One-way ANOVA revealed significant differences within amygdalar nuclei: basolateral amygdala, [BLA; $F(2,22) = 4.868$, $p = 0.0189$] and central nucleus [CeA; $F(2,22) = 10.48$, $p = 0.001$] (Fig. 5A, B). For both areas, post hoc analysis revealed significantly higher $\Delta FosB^+$ cell counts in CO_2-H mice relative to air controls ($p < 0.05$), while low responders to CO_2 (CO_2-L) were not significantly different from air or CO_2-H. Furthermore, significant group differences were noted within sub-regions of the medial prefrontal cortex suggestive of inverse activation patterns between the infralimbic and prelimbic cortex. ANOVA revealed significant effects of inhalation in the infralimbic subdivision [IL; $F(2,21) = 6.531$, $p = 0.007$) and prelimbic (PL; $F(2,19) = 6.787$, $p = 0.007$) cortices (Fig. 5C, D). Post hoc analyses revealed significantly reduced $\Delta FosB^+$ cell counts in CO_2-exposed mice as compared to air-exposed mice within the IL. Significantly higher cell counts were observed within the PL of CO_2-H mice versus air-exposed mice ($p < 0.05$), while CO_2-L mice were not different from the air group. Within the hippocampus ΔFosB immunostaining was confined to the dorsal dentate gyrus (dDG), where a significant effect of inhalation was observed [$F(2,19) = 1.36$, $p = 0.0334$] with CO_2 exposed mice showing reduced $\Delta FosB^+$ cell counts (Fig. 5E). Post hoc analysis revealed significantly lower $\Delta FosB^+$ cell counts in CO_2-L mice versus the air group. In contrast to the dorsal subdivision, the ventral hippocampus showed negligible $\Delta FosB^+$ cell counts (Fig. 5H). Significant group differences in $\Delta FosB^+$ cell counts were also observed within the bed nucleus of stria terminalis (BNST) (Fig. 5F) ($F(2,20) = 4.793$, $p = 0.021$), with significantly higher $\Delta FosB^+$ cell counts in CO_2-H mice relative to air controls ($p < 0.05$), while CO_2-L mice were not significantly different from either group. Despite a high density of $\Delta FosB^+$ cells within the NAc, there were no group differences (Fig. 5G), [$F(2,21) = 0.224$, $p = 0.802$).

Association of neuronal activation in cortico-dentate-amygdalar regions with fear conditioning and extinction behaviors

ΔFosB is a marker of persistent neuronal activation and may be associated with more than one behavior (as opposed to cFos). Correlation of regional $\Delta FosB^+$ cell counts with observed behaviors revealed region-specific associations with selective behaviors: contextual freezing in the fear conditioning test (Day 12) and extinction (mean freezing across days) (Table 2). As shown in Fig. 6A, a significant positive correlation between central amygdala, CeA $\Delta FosB^+$ cell counts and conditioned freezing was observed [CeA ($r = 0.545$, $p = 0.007$)]. Interestingly, dentate $\Delta FosB^+$ cell counts inversely correlated with conditioned freezing [dDG ($r = -0.419$, $p = 0.047$)] (Fig. 6A). $\Delta FosB^+$ cell counts within the IL subdivision showed a significant inverse correlation with mean extinction freezing [IL ($r = -0.524$, $p = 0.010$)] (Fig. 6B). Similarly, dentate $\Delta FosB^+$ cell counts also showed an inverse correlation with mean extinction freezing [dDG ($r = -0.473$, $p = 0.023$)] (Fig. 6B). No significant correlations between regional $\Delta FosB^+$ cell counts and other behaviors were observed including behavior during CO_2 and context exposure, startle response or fear acquisition and reinstatement (data not shown).

Disrupted cortico-dentate amygdalar co-activation patterns in CO_2-H mice

To further identify neural networks activated within this paradigm and to identify inter-regional co-activation patterns, correlation matrices of $\Delta FosB^+$ cell counts were visualized across regions for each group and examined as a proxy of functional connectivity between brain regions (Fig. 7). These maps revealed differential patterns of co-activation between groups. Most notable was the significant disruption of IL and dDG correlations with CeA, BLA, PL and BNST in CO_2-H mice. For example, inverse co-activation associations between IL-BLA and IL-PL observed in air and CO_2-L mice were significantly disrupted, becoming positive correlations in CO_2-sensitive mice. Furthermore, CO_2-H mice also elicited positive dDG-amygdala and dDG-BNST co-activation patterns that were not observed in the other groups. Interestingly, distinct patterns in co-activation are also apparent in the CO_2-L cohort such as a strong negative dDG-PL and IL-PL association that was not observed in air or CO_2-H groups.

DISCUSSION

Overall, our data support an association of behavioral sensitivity to CO_2 with potentiated fear memory as well as disrupted forebrain neuronal activation.

The observation that sensitivity to a homeostatic threat (CO_2 inhalation) can have long lasting effects on fear memory to an external (exteroceptive) trigger, footshocks, is intriguing. Relevance of the homeostatic state and interoceptive signals in shaping behavior has long been recognized (Damasio and Carvalho, 2013), and there is significant interest in how homeostatic and interoceptive processes integrate with emotional regulation and mental health (Khalsa et al., 2018). Fluctuations in the internal milieu that signal a threat to homeostasis can modulate defensive behaviors, however, contributory mechanisms are not clear. Rising CO_2 concentrations constitute a threat to homeostasis and elicit intense fear (Gorman et al., 2001; Colasanti et al., 2008). CO_2 is a cross-species experimental

trigger of panic-relevant behaviors (Ziemann et al., 2009; Taugher et al., 2014; Vollmer et al., 2015; Leibold et al., 2016; Battaglia, 2017) and recent reports demonstrate increased CO_2-sensitivity in PTSD subjects (Muhtz et al., 2012; Kellner et al., 2018). Interestingly, panic and PTSD are often comorbid suggestive of shared vulnerability factors. Together with prior studies, the data presented here suggest CO_2 sensitivity may represent one shared vulnerability factor of great relevance in the study of panic and PTSD risk.

Interestingly, these data also suggest that CO_2 inhalation may identify vulnerable populations and predict later responses to exteroceptive triggers of relevance to PTSD. Prior response to CO_2 inhalation was significantly correlated with fear extinction behavior and CO_2-H mice demonstrated enhanced conditioned fear and delayed fear extinction suggesting altered fear regulatory mechanisms in these animals. The lack of significant group differences in acoustic startle, freezing during pre-shock habituation period and fear acquisition suggests that prior CO_2 exposure does not result in a generalized fear sensitization effect, but that effects may be selective to fear memory. In agreement with these observations a recent study reported significant interaction effects of CO_2 inhalation on extinction in rats (Monfils et al., 2018) suggesting the utility of CO_2 inhalation as an interoceptive stressor associated with fear deficits across species.

Since we did not assess pre-CO_2 factors in this study to avoid confounding effects on subsequent behaviors, it is not clear what mechanisms may promote differential CO_2 responding. While we would expect BALB/c mice (inbred strain) to show less dichotomous responses than outbred mice, individual differences do exist within inbred strains of mice as a result of either environmental effects or gene by environment interactions (Lathe, 2004; Loos et al., 2015). Examples of uncontrollable environmental factors include intrauterine position of the embryo, feeding hierarchy in newborns, and imprinting errors (Lathe, 2004). Additionally, some genetic variation could exist due to de novo mutations or copy number variations (Egan et al., 2007). These prior effects or random mutations could have lasting effects on a variety of CO_2-chemosensory mechanisms which may have contributed to the variation in CO_2 response and altered fear extinction. For example, early life stress is known to regulate expression of acid sensing ion channels (ASICs) and is associated with CO_2 hypersensitivity and increased nociception (Cittaro et al., 2016; Battaglia et al., 2018). The impact of early life adversity on both CO_2 sensitivity and nociception further suggest a role of shared risk factors contributing to interoceptive and exteroceptive threat responses and potential overlapping regulatory mechanisms. The acid sensing G protein receptor, TDAG8 (Vollmer et al., 2016) also appears to be relevant given the large variance in TDAG8 expression observed in humans (Strawn et al., 2018). In previous studies we reported altered serotonergic and noradrenergic cell counts between high and low CO_2-sensitive rat strains (Winter et al., 2017) consistent with other observations (Bailey et al., 2003; Leibold et al., 2015), and it is possible that these systems also contribute to differential behavioral sensitivity to CO_2 in mice. A recent study reported an association of orexin neurons in the lateral hypothalamic area with variability in CO_2 reactivity as well as modulation of long-term fear memory (Monfils et al., 2018). Lastly, neuroimmune factors may also contribute to variable CO_2 sensitivity as we previously reported a contribution of microglial and pro-inflammatory cytokines in CO_2-evoked fear (Vollmer et al., 2016). Interestingly, contribution of inflammatory dysfunction has been proposed as a preceding

risk factor for fear-related disorders such as PTSD (Deslauriers et al., 2017). It would be important to investigate the association of these factors with CO_2 sensitivity and delayed fear potentiation.

Post behavior ΔFosB mapping, a measure of persistent neuronal activation, provides important insights on potential regional/circuit alterations that may have contributed to observed behavioral differences. Significant effects of CO_2 inhalation on neuronal activation were observed in forebrain subregions regulating contextual fear and extinction including dDG, CeA, BLA, PL, IL, and BNST. These highly interconnected areas regulate unconditioned and conditioned defensive behaviors (Davis et al., 2010; Sierra-Mercado et al., 2011a; Lebow and Chen, 2016), house chemosensory mechanisms (Ziemann et al., 2009; Taugher et al., 2014), receive afferents from several homeostatic regulatory nodes (Miselis, 1981; Damasio and Carvalho, 2013; Johnson et al., 2014; Tye, 2018) and have been implicated in fear disorders such as PTSD (Gorman et al., 2000). We observed the strongest association of context conditioned freezing with neuronal activation within the dDG and CeA which is consistent with their well-established role in contextual fear memory regulation (Izquierdo et al., 2016). An inverse correlation of conditioned freezing and dDG $\Delta FosB^+$ cell counts (suggesting reduced dDG activation in enhanced fear) is consistent with previous studies reporting that optimal neuronal activation within the DG is desirable for conditioned fear expression (Eagle et al., 2015). In contrast, a positive association of CeA activation with conditioned freezing was observed, consistent with the well-established role of this site in learning-memory and expression of fear (Keifer et al., 2015).

An association of reduced activation of the IL with increased extinction freezing is consistent with the well-recognized role of this region regulation of extinction (Sierra-Mercado et al., 2011b; Do-Monte et al., 2015), and the association of IL dysfunction with extinction deficits (Milad et al., 2007; Arruda-Carvalho and Clem, 2015). Our data also supports a contribution of reduced dDG activation to high extinction freezing. This observation is in agreement with a recent optogenetic study where suppressed DG activation resulted in compromised extinction (Bernier et al., 2017).

Regional co-activation mapping reveals information about potential neurocircuits that may have contributed to behavioral sensitivity in CO_2-H mice. Observed disruption in cortico-amygdala, DG-amygdala and intra-cortical activation patterns in CO_2-H mice may contribute to increased conditioned fear and delayed extinction in these animals. An inverse IL-BLA co-activation pattern is observed in air and CO_2-L mice, consistent with the top-down control of the amygdala by IL which promotes extinction learning, retention and retrieval (Baldi and Bucherelli, 2015; Giustino and Maren, 2015). This association appears to be disrupted in CO_2-H mice, consistent with the observed deficits in extinction learning in these animals. In addition to the IL-BLA, inverse dDG and CeA/BLA co-activation patterns were observed in CO_2-L and air mice. Interactions between the hippocampus and amygdala promote regulation of fear by contextual cues. Previous studies have reported that the hippocampus drives prefrontal cortex inhibition of the amygdala to suppress fear (Hobin et al., 2003; Maren and Quirk, 2004). These associations were altered in CO_2-H mice. Altered co-activation patterns between IL and PL subdivisions of the medial PFC were also observed in CO_2-H mice. Multiple lines of evidence suggest a functional dichotomy

between the PL and IL in regulation of expression and suppression of fear, respectively [reviewed in (Giustino and Maren, 2015)]. Consistent with this, low CO_2 responders showed an inverse IL-PL activation pattern while this association was disrupted in CO_2-H mice. Overall, disruptions in the coordinated activity of cortico-hippocampal-amygdalar areas in CO_2-sensitive mice may explain the increased fear phenotype of this group.

Though the behavior is similar between Air and CO_2-L groups, post hoc tests did not reveal significant differences in ΔFosB+ cell counts between CO_2-L and air or CO_2-H groups. Although ΔFosB immunostaining provides valuable information about contribution of potential brain areas in observed behaviors, it does not inform on which cell phenotypes represent immunostaining. It is possible that separate neuronal populations engage in CO_2-L mice facilitating a “resilient” behavioral phenotype that is distinct from air and CO_2-H mice, where these mice respond differently to the homeostatic stressor CO_2, rather than not responding at all. This is further supported by the co-activation matrices (Fig. 7) which show distinct patterns of co-activation within all three groups, with the CO_2-L and Air groups showing differential patterns in some brain areas. It would be important to determine underlying mechanisms that distinguish these cohorts.

Our study assessed CO_2 sensitivity using behavioral readouts and focused on unconditioned (startle) and conditioned (fear conditioning) behaviors relevant to PTSD. However, it would be important to determine if CO_2-evoked physiological responses (hyperventilation, cardiovascular activation) also associate with delayed emergence of sensitized fear and startle. Pre-CO_2 factors that may have contributed to variation in behavioral sensitivity to CO_2 are not evident. In this investigation, stress was not investigated as a variable since the objective was to determine CO_2-fear-startle associations, however, it would be important to investigate the interaction of stress and traumatic exposures with CO_2 inhalation. Our tissue analyses was confined to post-behavior measurements, however, it would be important to investigate the trajectory of early-onset CO_2-evoked alterations and how they translate to dysregulated behaviors and altered forebrain circuitry.

In recent years, the value of investigating mechanisms promoting individual differences in behavioral responding has been recognized. Previous studies suggest pre-trauma biological and cognitive vulnerability factors that might place individuals at risk for PTSD development (Bomyea et al., 2012). Our findings relate to a previous clinical study where sensitivity to CO_2 was identified as a pre-deployment vulnerability factor associated with increased combat stress reactions and posttraumatic symptomology in soldiers deployed to the war zone (Telch et al., 2012). In another study, panic attacks were a strong predictor of PTSD symptom severity (Cougle et al., 2010), although CO_2 sensitivity was not investigated. Collectively, our findings in conjunction with previous evidence suggests that CO_2 hypersensitivity may be a pre-morbid risk factor for the development of PTSD. CO_2 hypersensitivity may also represent a pathophysio-logical phenotype in panic-PTSD comorbidity where sensitized reactivity to interoceptive and exteroceptive cues may collectively result in panic attacks, hyperarousal and intrusive trauma-associated fear memories.

In conclusion, our data highlight an association of prior interoceptive experiences in shaping long term individual differences in fear behaviors. Sensitivity to interoceptive threats such as CO_2 may promote inter-individual variability rendering “sensitive” individuals susceptible to developing PTSD and comorbid panic-PTSD.

ACKNOWLEDGEMENTS

This research was supported by VA Merit award 2I01BX001075 (RS). KMJM acknowledges support from NIH postdoctoral training grants T32DK059803 and F32MH117913. Technical assistance from Ms. Jennifer Schurdak is also acknowledged. KMJM and RS designed the study, KMJM and AJ collected data, KMJM, PH and RS analyzed data, KMJM and RS interpreted data and wrote the manuscript.

Abbreviations:

BLA	basolateral amygdala
BNST	bed nucleus of stria terminalis
CeA	central amygdala
CO2-H	carbon dioxide high responders
CO2-L	carbon dioxide high responders
dDG	dorsal dentate gyrus of the hippocampus
IHC	immunohistochemistry
IL	infralimbic cortex
mPFC	medial prefrontal cortex
NAc	nucleus accumbens
PL	prelimbic cortex
PTSD	post-traumatic stress disorder
vDG	ventral dentate gyrus of the hippocampus
ΔFosB	delta FosB
ΔFosB	ΔFosB immunopositive cell counts

REFERENCES

Arruda-Carvalho M, Clem RL (2015) Prefrontal-amygdala fear networks come into focus. Front Syst Neurosci 9:145. [PubMed: 26578902]

Bailey JE, Argyropoulos SV, Lightman SL, Nutt DJ (2003) Does the brain noradrenaline network mediate the effects of the CO2 challenge? J Psychopharmacol 17:267–268.

Baldi E, Bucherelli C (2015) Brain sites involved in fear memory reconsolidation and extinction of rodents. Neurosci Biobehav Rev 53:160–190. [PubMed: 25887284]

Battaglia M (2017) Sensitivity to carbon dioxide and translational studies of anxiety disorders. Neuroscience 346:434–436. [PubMed: 28188857]

Battaglia M, Rossignol O, Bachand K, D'Amato FR, De Koninck Y (2018) Amiloride modulation of carbon dioxide hypersensitivity and thermal nociceptive hypersensitivity induced by interference with early maternal environment. J Psychopharmacol 33 (1):101–108. [PubMed: 29968500]

Bernier BE, Lacagnina AF, Ayoub A, Shue F, Zemelman BV, Krasne FB, Drew MR (2017) Dentate gyrus contributes to retrieval as well as encoding: evidence from context fear conditioning, recall, and extinction. J Neurosci 37:6359–6371. [PubMed: 28546308]

Boettcher H, Brake CA, Barlow DH (2016) Origins and outlook of interoceptive exposure. J Behav Ther Exp Psychiatry 53:41–51. [PubMed: 26596849]

Bomyea J, Risbrough V, Lang AJ (2012) A consideration of select pre-trauma factors as key vulnerabilities in PTSD. Clin Psychol Rev 32:630–641. [PubMed: 22917742]

Cittaro D, Lampis V, Luchetti A, Coccurello R, Guffanti A, Felsani A, Moles A, Stupka E, D'Amato FR, Battaglia M (2016) Histone modifications in a mouse model of early adversities and panic disorder: role for asic1 and neurodevelopmental genes. Sci Rep 6:25131. [PubMed: 27121911]

Colasanti A, Salamon E, Schruers K, van Diest R, van Duinen M, Griez EJ (2008) Carbon dioxide-induced emotion and respiratory symptoms in healthy volunteers. Neuropsychopharmacology 33:3103–3110. [PubMed: 18354390]

Cougle JR, Feldner MT, Keough ME, Hawkins KA, Fitch KE (2010) Comorbid panic attacks among individuals with posttraumatic stress disorder: associations with traumatic event exposure history, symptoms, and impairment. J Anxiety Disord 24:183–188. [PubMed: 19914036]

Craig AD (2002) How do you feel? Interoception: the sense of the physiological condition of the body. Nat Rev Neurosci 3:655–666. [PubMed: 12154366]

Craig AD (2003) Interoception: the sense of the physiological condition of the body. Curr Opin Neurobiol 13:500–505. [PubMed: 12965300]

Damasio A, Carvalho GB (2013) The nature of feelings: evolutionary and neurobiological origins. Nat Rev Neurosci 14:143–152. [PubMed: 23329161]

Davis M, Walker DL, Miles L, Grillon C (2010) Phasic vs sustained fear in rats and humans: role of the extended amygdala in fear vs anxiety. Neuropsychopharmacology 35:105–135. [PubMed: 19693004]

Deslauriers J, Powell SB, Risbrough VB (2017) Immune signaling mechanisms of PTSD risk and symptom development: insights from animal models. Curr Opin Behav Sci 14:123–132. [PubMed: 28758144]

Do-Monte FH, Manzano-Nieves G, Quinones-Laracuente K, Ramos-Medina L, Quirk GJ (2015) Revisiting the role of infralimbic cortex in fear extinction with optogenetics. J Neurosci 35:3607–3615. [PubMed: 25716859]

Eagle AL, Gajewski PA, Yang M, Kechner ME, Al Masraf BS, Kennedy PJ, Wang H, Mazei-Robison MS, Robison AJ (2015) Experience-dependent induction of hippocampal ΔFosB controls learning. J Neurosci 35:13773–13783. [PubMed: 26446228]

Egan CM, Sridhar S, Wigler M, Hall IM (2007) Recurrent DNA copy number variation in the laboratory mouse. Nat Genet 39:1384–1389. [PubMed: 17965714]

Etkin A, Wager TD (2007) Functional neuroimaging of anxiety: a meta-analysis of emotional processing in PTSD, social anxiety disorder, and specific phobia. Am J Psychiatry 164:1476–1488. [PubMed: 17898336]

Giustino TF, Maren S (2015) The role of the medial prefrontal cortex in the conditioning and extinction of fear. Front Behav Neurosci 9:298. [PubMed: 26617500]

Gorman JM, Kent J, Martinez J, Browne S, Coplan J, Papp LA (2001) Physiological changes during carbon dioxide inhalation in patients with panic disorder, major depression, and premenstrual dysphoric disorder: evidence for a central fear mechanism. Arch Gen Psychiatry 58:125–131. [PubMed: 11177114]

Gorman JM, Kent JM, Sullivan GM, Coplan JD (2000) Neuroanatomical hypothesis of panic disorder, revised. Am J Psychiatry 157:493–505. [PubMed: 10739407]

Hobin JA, Goosens KA, Maren S (2003) Context-dependent neuronal activity in the lateral amygdala represents fear memories after extinction. J Neurosci 23:8410–8416. [PubMed: 12968003]

Izquierdo I, Furini CRG, Myskiw JC (2016) Fear memory. Physiol Rev 96:695–750. [PubMed: 26983799]

Johnson PL, Federici LM, Shekhar A (2014) Etiology, triggers and neurochemical circuits associated with unexpected, expected, and laboratory-induced panic attacks. Neurosci Biobehav Rev 46 (Pt 3):429–454. [PubMed: 25130976]

Keifer OP, Hurt RC, Ressler KJ, Marvar PJ (2015) The physiology of fear: reconceptualizing the role of the central amygdala in fear learning. Physiology 30:389–401. [PubMed: 26328883]

Kellner M, Muhtz C, Nowack S, Leichsenring I, Wiedemann K, Yassouridis A (2018) Effects of 35% carbon dioxide (CO 2) inhalation in patients with post-traumatic stress disorder (PTSD): a double-blind, randomized, placebo-controlled, cross-over trial. J Psychiatr Res 96:260–264. [PubMed: 29128558]

Kessler RC, Sonnega A, Bromet E, Hughes M, Nelson CB (1995) Posttraumatic stress disorder in the National Comorbidity Survey. Arch Gen Psychiatry 52:1048–1060. [PubMed: 7492257]

Khalsa SSet al. (2018) Interoception and mental health: a roadmap. Biol Psychiatry Cogn Neurosci Neuroimaging 3:501–513. [PubMed: 29884281]

Koenigs M, Huey ED, Raymont V, Cheon B, Solomon J, Wassermann EM, Grafman J (2008) Focal brain damage protects against post-traumatic stress disorder in combat veterans. Nat Neurosci 11:232–237. [PubMed: 18157125]

Lathe R (2004) The individuality of mice. Genes Brain Behav 3:317–327. [PubMed: 15544575]

Lebow MA, Chen A (2016) Overshadowed by the amygdala: the bed nucleus of the stria terminalis emerges as key to psychiatric disorders. Mol Psychiatry 21:450–463. [PubMed: 26878891]

Leibold NK, van den Hove DLA, Esquivel G, De Cort K, Goossens L, Strackx E, Buchanan GF, Steinbusch HWM, Lesch KP, Schruers KRJ (2015) The brain acid-base homeostasis and serotonin: a perspective on the use of carbon dioxide as human and rodent experimental model of panic. Prog Neurobiol 129:58–78. [PubMed: 25930682]

Leibold NK, van den Hove DLA, Viechtbauer W, Buchanan GF, Goossens L, Lange I, Knuts I, Lesch KP, Steinbusch HWM, Schruers KRJ (2016) CO2 exposure as translational cross-species experimental model for panic. Transl Psychiatry 6 e885. [PubMed: 27598969]

Liberzon I, Abelson JL (2016) Context processing and the neurobiology of post-traumatic stress disorder. Neuron 92:14–30. [PubMed: 27710783]

Lisieski MJ, Eagle AL, Conti AC, Liberzon I, Perrine SA (2018) Single-prolonged stress: a review of two decades of progress in a rodent model of posttraumatic stress disorder. Front Psychiatry 9:196. [PubMed: 29867615]

Loos M, Koopmans B, Aarts E, Maroteaux G, van der Sluis S, M Neuro-BSIK Mouse Phenomics Consortium, Verhage M, Smit AB (2015) Within-strain variation in behavior differs consistently between common inbred strains of mice. Mamm Genome 26:348–354. [PubMed: 26123533]

Maren S, Phan KL, Liberzon I (2013) The contextual brain: implications for fear conditioning, extinction and psychopathology. Nat Rev Neurosci 14:417–428. [PubMed: 23635870]

Maren S, Quirk GJ (2004) Neuronal signalling of fear memory. Nat Rev Neurosci 5:844–852. [PubMed: 15496862]

McGuire J, Herman JP, Horn PS, Sallee FR, Sah R (2010) Enhanced fear recall and emotional arousal in rats recovering from chronic variable stress. Physiol Behav 101:474–482. [PubMed: 20678511]

McMurray KMJ, Strawn JR, Sah R (2019) Fluoxetine modulates spontaneous and conditioned behaviors to carbon dioxide (CO_2) inhalation and alters forebrain-midbrain neuronal activation. Neuroscience 396:108–118. [PubMed: 30439538]

Michopoulos V, Powers A, Gillespie CF, Ressler KJ, Jovanovic T (2017) Inflammation in fear- and anxiety-based disorders: PTSD, GAD, and beyond. Neuropsychopharmacology 42:254–270. [PubMed: 27510423]

Milad MR, Wright CI, Orr SP, Pitman RK, Quirk GJ, Rauch SL (2007) Recall of fear extinction in humans activates the ventromedial prefrontal cortex and hippocampus in concert. Biol Psychiatry 62:446–454. [PubMed: 17217927]

Miselis RR (1981) The efferent projections of the subfornical organ of the rat: a circumventricular organ within a neural network subserving water balance. Brain Res 230:1–23. [PubMed: 7317773]

Monfils MH, Lee HJ, Keller NE, Roquet RF, Quevedo S, Agee L, Cofresi R, Shumake J (2018) Predicting extinction phenotype to optimize fear reduction. Psychopharmacology (Berl) 236:99–110. [PubMed: 30218131]

Moreno-Fernández RD, Pérez-Martín M, Castilla-Ortega E, Rosell del Valle C, García-Fernández MI, Chun J, Estivill-Torrús G, Rodríguez de Fonseca F, Santín LJ, Pedraza C (2017) maLPA1-null mice as an endophenotype of anxious depression. Transl Psychiatry 7 e1077. [PubMed: 28375206]

Morgan CA, Grillon C, Southwick SM, Davis M, Charney DS (2015) Fear-potentiated startle in posttraumatic stress disorder. Biol Psychiatry:1–8.

Muhtz C, Wiedemann K, Kellner M (2012) Panicogens in patients with Post-Traumatic Stress Disorder (PTSD). Curr Pharm Des 18:5608–5618. [PubMed: 22632476]

Muhtz C, Yassouridis A, Daneshi J, Braun M, Kellner M (2011) Acute panicogenic, anxiogenic and dissociative effects of carbon dioxide inhalation in patients with post-traumatic stress disorder (PTSD). J Psychiatr Res 45:989–993. [PubMed: 21324483]

Ross DA, Arbuckle MR, Travis MJ, Dwyer JB, van Schalkwyk GI, Ressler KJ (2017) An integrated neuroscience perspective on formulation and treatment planning for posttraumatic stress disorder. JAMA Psychiatry 74:407. [PubMed: 28273291]

Schubert I, Ahlbrand R, Winter A, Vollmer L, Lewkowich I, Sah R (2018) Enhanced fear and altered neuronal activation in forebrain limbic regions of CX3CR1-deficient mice. Brain Behav Immun 68:34–43. [PubMed: 28943292]

Sierra-Mercado D, Padilla-Coreano N, Quirk GJ (2011) Dissociable roles of prelimbic and infralimbic cortices, ventral hippocampus, and basolateral amygdala in the expression and extinction of conditioned fear. Neuropsychopharmacology 36:529–538. [PubMed: 20962768]

Strawn JR, Vollmer LL, McMurray KMJ, Mills JA, Mossman SA, Varney ST, Schroeder HK, Sah R (2018) Acid-sensing T cell death associated gene-8 receptor expression in panic disorder. Brain Behav Immun 67:36–41. [PubMed: 28736033]

Taugher RJ, Lu Y, Wang Y, Kreple CJ, Ghobbeh A, Fan R, Sowers LP, Wemmie JA (2014) The bed nucleus of the stria terminalis is critical for anxiety-related behavior evoked by CO2 and acidosis. J Neurosci 34:10247–10255. [PubMed: 25080586]

Telch MJ, Rosenfield D, Lee H-J, Pai A (2012) Emotional reactivity to a single inhalation of 35% carbon dioxide and its association with later symptoms of posttraumatic stress disorder and anxiety in soldiers deployed to Iraq. Arch Gen Psychiatry 69:1161–1168. [PubMed: 23117637]

Thomas JL, Wilk JE, Riviere LA, McGurk D, Castro CA, Hoge CW (2010) Prevalence of mental health problems and functional impairment among active component and national guard soldiers 3 and 12 months following combat in Iraq. Arch Gen Psychiatry 67:614. [PubMed: 20530011]

Tye KM (2018) Neural circuit motifs in valence processing. Neuron 100:436–452. [PubMed: 30359607]

Vollmer L, Ghosal S, A Rush J, R Sallee F, P Herman J, Weinert M, Sah R (2013) Attenuated stress-evoked anxiety, increased sucrose preference and delayed spatial learning in glucocorticoid-induced receptor-deficient mice. Genes Brain Behav 12:241–249. [PubMed: 23088626]

Vollmer LL, Strawn JR, Sah R (2015) Acid-base dysregulation and chemosensory mechanisms in panic disorder: a translational update. Transl Psychiatry:5.

Vollmer LL, Ghosal S, McGuire JL, Ahlbrand RL, Li K-Y, Santin JM, Ratliff-Rang CA, Patrone LGA, Rush J, Lewkowich IP, Herman JP, Putnam RW, Sah R (2016) Microglial acid sensing regulates carbon dioxide-evoked fear. Biol Psychiatry 80:541–551. [PubMed: 27422366]

Whitaker AM, Gilpin NW, Edwards S (2014) Animal models of post-traumatic stress disorder and recent neurobiological insights. Behav Pharmacol 25:398–409. [PubMed: 25083568]

Winter A, Ahlbrand R, Naik D, Sah R (2017) Differential behavioral sensitivity to carbon dioxide (CO2) inhalation in rats. Neuroscience.

Winter A, Ahlbrand R, Sah R (2019) Recruitment of central angiotensin II type 1 receptor associated neurocircuits in carbon dioxide associated fear. Prog Neuro-Psychopharmacology Biol Psychiatry 92:378–386.

Ziemann AE, Allen JE, Dahdaleh NS, Drebot II, Coryell MW, Wunsch AM, Lynch CM, Faraci FM, Howard MA, Welsh MJ, Wemmie JA (2009) The amygdala is a chemosensor that detects carbon dioxide and acidosis to elicit fear behavior. Cell 139:1012–1021. [PubMed: 19945383]

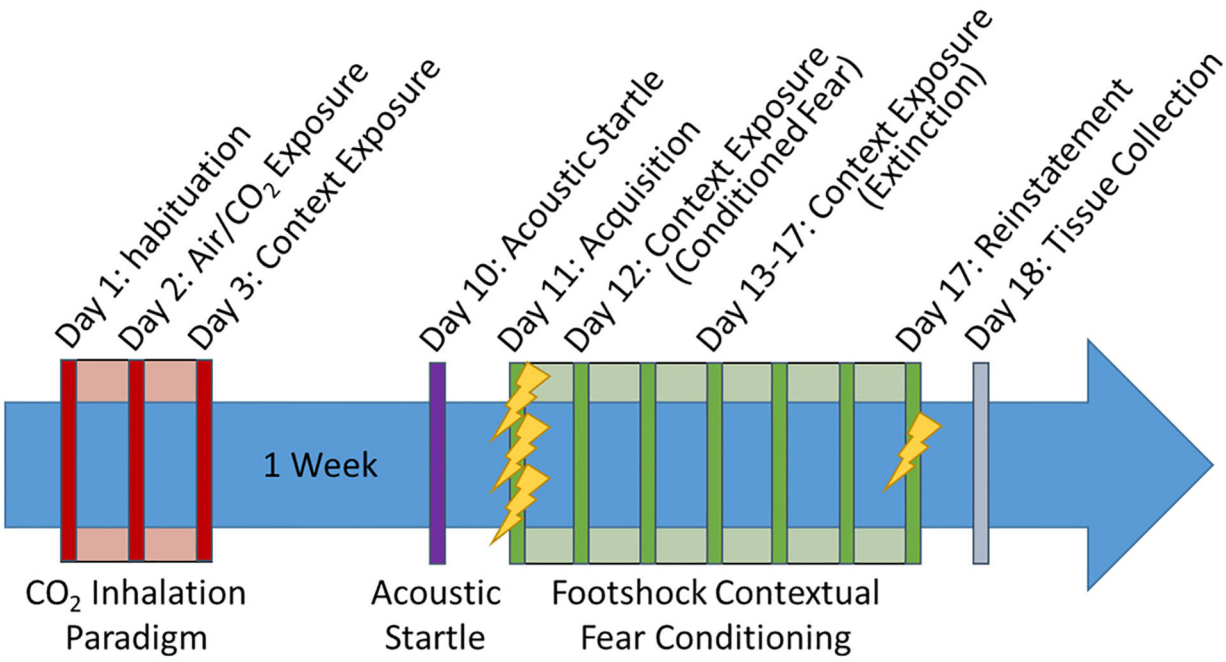

Fig. 1.

Timeline of study: following habituation to the CO_2 chamber (Day 1) mice were exposed to CO_2 or Air inhalation for 10 min (Day 2) and followed by re-exposure to context on Day 3. After a 1-week rest period, mice were tested for reactivity to exteroceptive stimuli in the form of acoustic startle (Day 10) followed by a contextual fear conditioning paradigm (Day 11–17). Mice were administered three footshocks for fear acquisition (Day 11), then exposed to context after 24 h for testing conditioned fear expression (Day 12), followed by repeated context exposure for extinction (Days 13–17). After the final extinction session mice were administered a single reminder shock to test fear reinstatement (Day 17). One cohort was sacrificed 24 h post behavior (Day 18) and brains collected for delta FosB (ΔFosB) immunostaining as a readout of persistent neuronal activation.

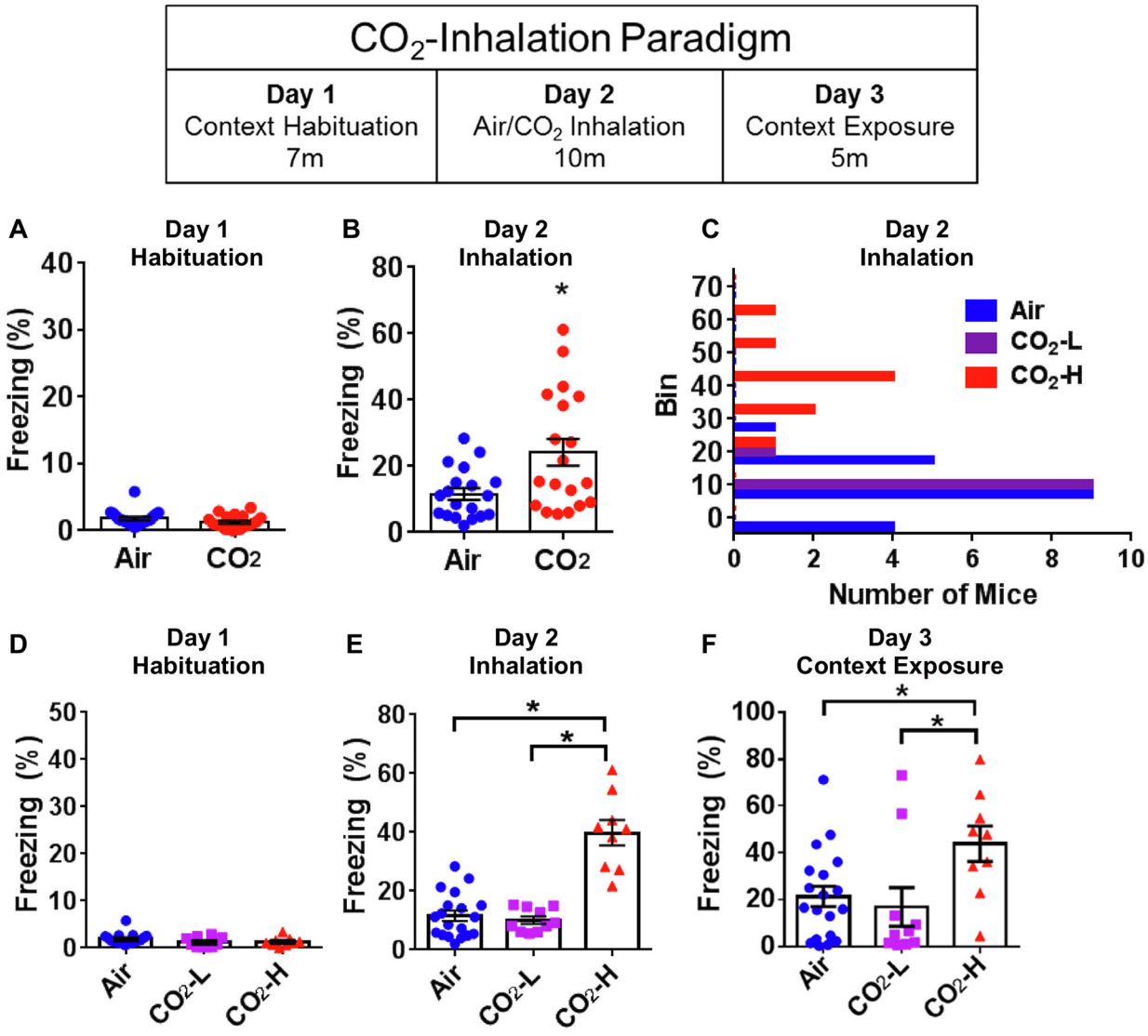

Fig. 2.

CO_2 inhalation evokes differential freezing behavior in mice. Mice were exposed to the CO_2 inhalation paradigm (see layout) comprising of habituation (**A**, **D**), CO_2 inhalation (**B**, **C** and **E**) and context exposure (**F**). (**A**) No differences in freezing during habituation to context on Day 1 in mice exposed to air or CO_2. (**B**) Significantly higher freezing was observed in mice exposed to CO_2 in comparison with the air cohort on Day 2. (**C**) A frequency distribution histogram of Day 2 freezing revealed subpopulations within the CO_2-exposed mice, with a group showing freezing behavior that largely overlapped with air exposed mice (CO_2-low, CO_2-L) and the other separated by higher freezing (CO_2-high, CO_2-H). (**D**) Dichotomization using a median split showed no significant group differences during habituation (Day 1). (**E**) During air or CO_2 inhalation (Day 2), CO_2-H mice showed significantly higher freezing in comparison to both air and CO_2-L groups and no differences between air and CO_2-L cohorts. (**F**) Exposure to context on Day 3 shows significantly higher freezing in the CO_2-H

group as compared to air and CO_2-L mice. Data are represented as mean ± SEM; *p < 0.05 versus air group or CO_2-L group (N = 9–19 mice per group).

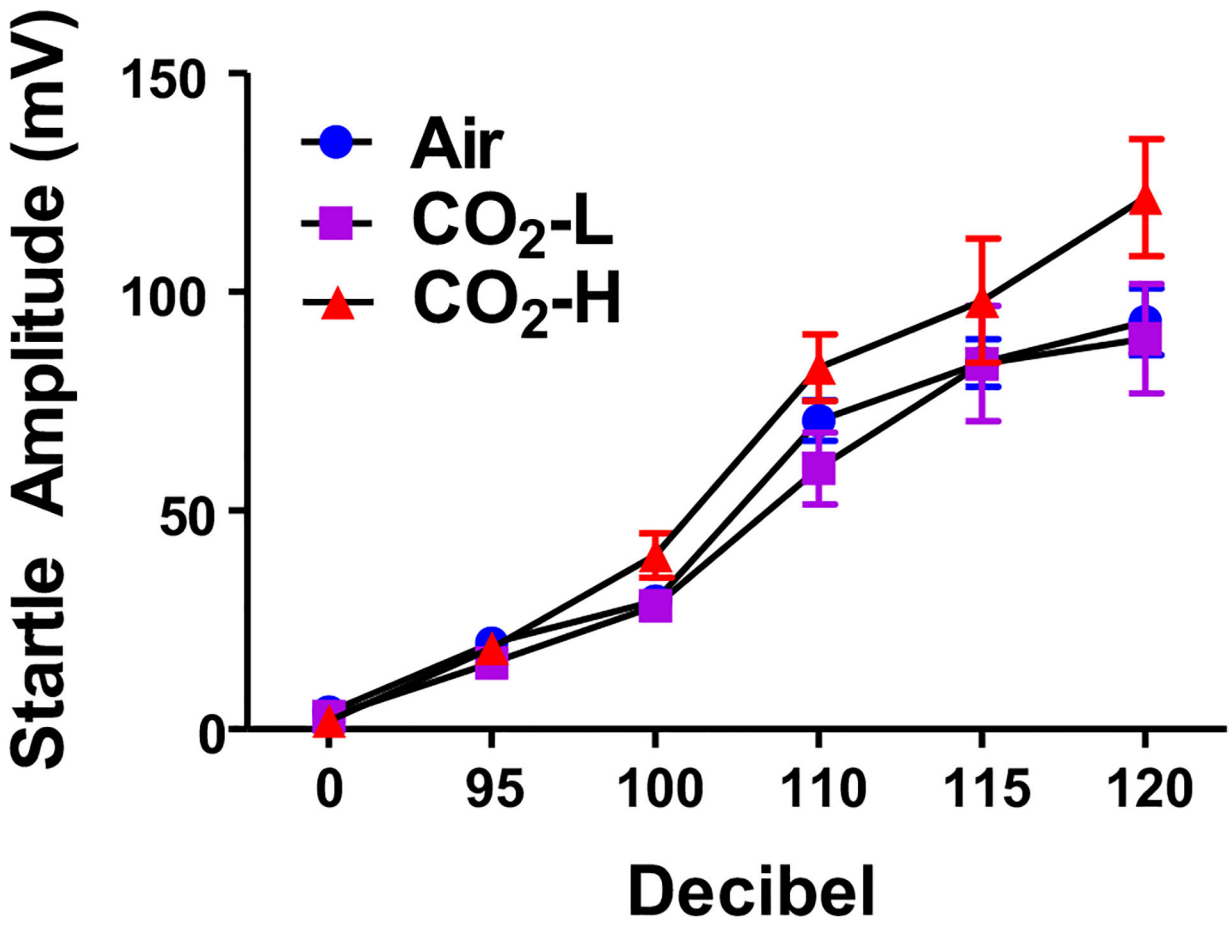

Fig. 3.

Mean startle amplitude in air, CO_2-L and CO_2-H mice to a range of acoustic stimuli ranging across 95, 100, 110 and 120 db is presented. Significant effects of decibel but no significant effects of inhalation were noted.

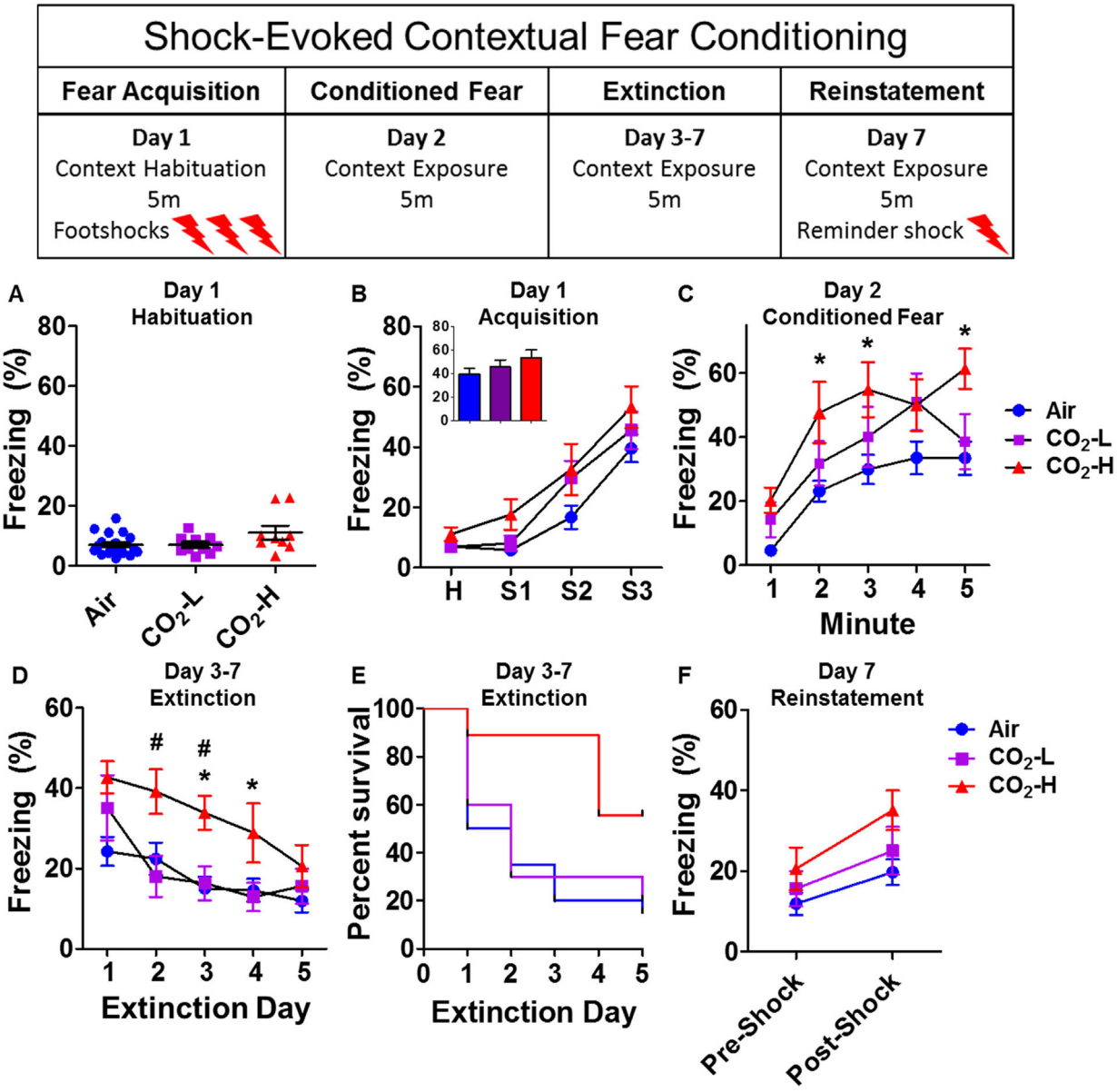

Fig. 4.

Enhanced fear conditioning and delayed extinction in CO_2-H mice. Mice were exposed to a contextual fear conditioning paradigm (see layout). (**A**) No significant group differences in freezing were observed during pre-shock context habituation. (**B**) No significant group differences in overall freezing were observed after footshocks (*H* = 5 min avg of habituation freezing; S1–S3 = shock 1 through 3) during fear acquisition. Mean freezing after final shock was not significantly different between groups (**B** inset). (**C**) On exposure to shock context 24 h post acquisition, CO_2-H mice showed significantly higher conditioned freezing as compared with the air group. (**D**) Mice were re-exposed to the acquisition context for extinction of fear for 5 days (1–5). CO_2-H mice showed delayed extinction learning with significantly higher freezing as compared to both air and CO_2-L mice on extinction days 2, 3 and 4. (**E**) Survival curves of extinction learning illustrate that CO_2-H mice took

significantly longer to reach criterion (freezing below 15%). (**F**) No significant differences in freezing were observed between groups after a single reminder shock for reinstatement of fear. Data are mean ± SEM; *p < 0.05 versus air; $^{\#}p < 0.05$ versus CO_2-L group, ($N = 9–19$ mice per group).

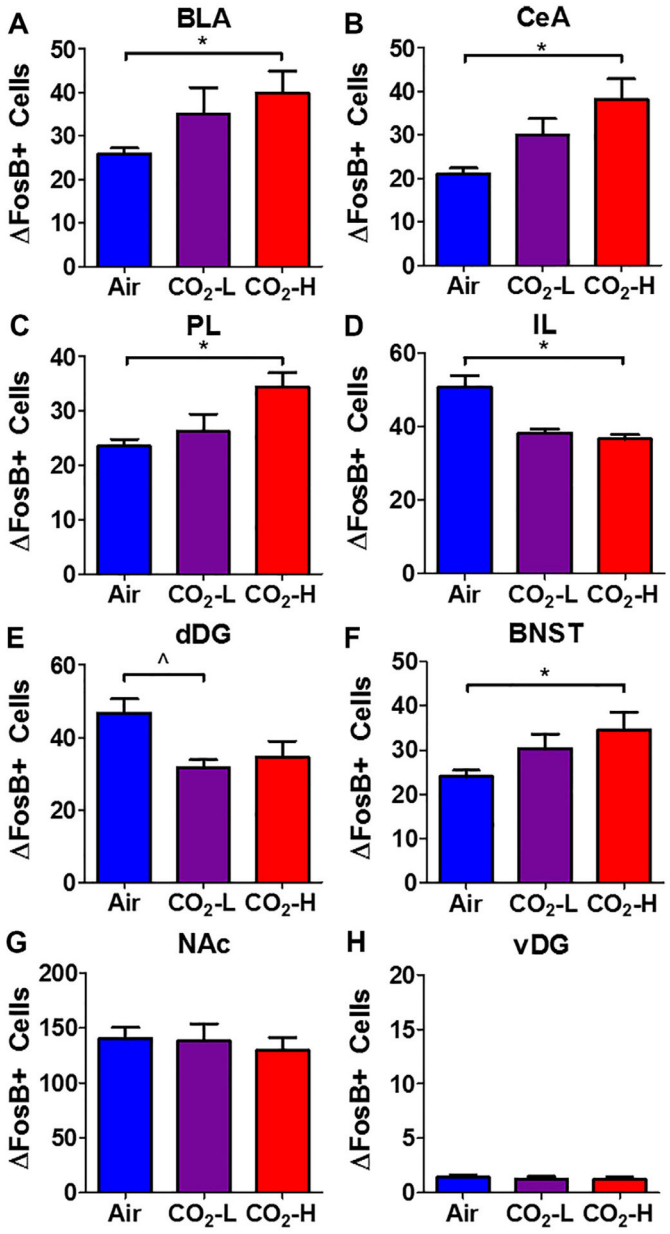

Fig. 5.

Regional ΔFosB+ cell counts in air, CO_2-L and CO_2-H mice. Significant alterations in ΔFosB+ cell counts were observed in multiple brain areas: Increased cell counts were observed in (**A**) basolateral amygdala (BLA), (**B**) central nucleus of amygdala (CeA), (**C**) prelimbic cortex (PL), (**F**) bed nucleus of stria terminalis (BNST) of CO_2-H mice. (**D**) Significantly reduced cell counts were observed in CO_2-H mice within the infralimbic cortex (IL). (**E**) Reductions were also observed within the dorsal dentate gyrus (dDG). No significant differences were noted within the (**G**) nucleus accumbens (NAc) and (**H**) ventral dentate gyrus (vDG). Data are mean ± SEM. *$p < 0.05$ CO_2-H versus air, $p < 0.05$ CO_2-L versus air.

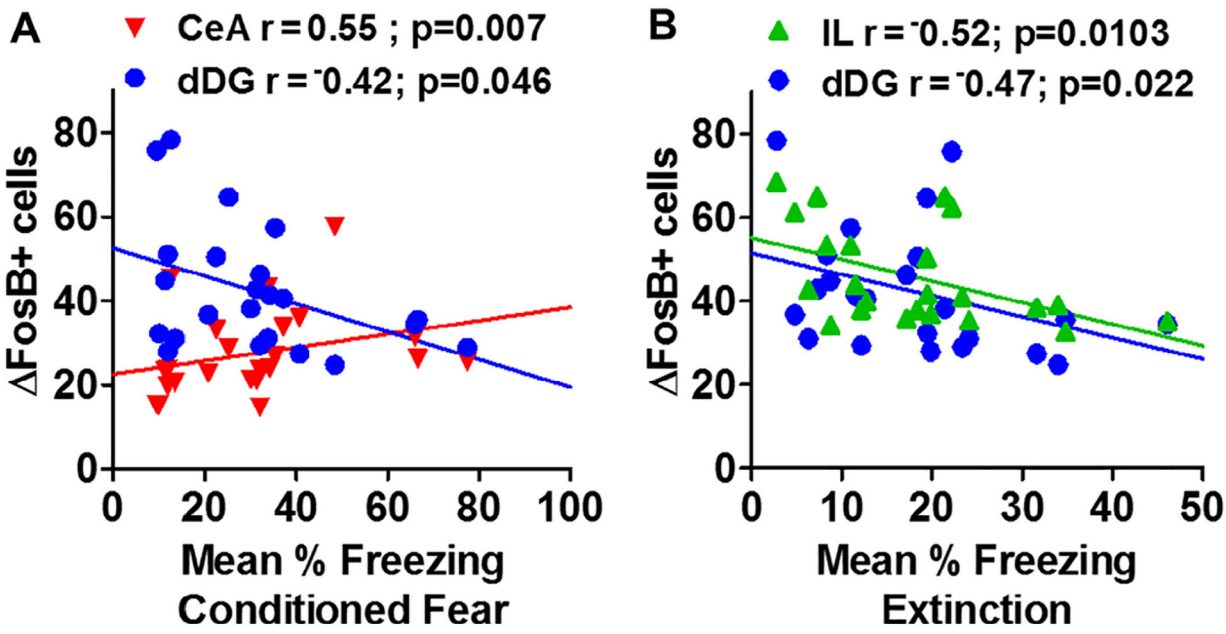

Fig. 6.

Neuronal activation within hippocampus-amygdala-cortical subregions associates with freezing during conditioned fear and extinction of the contextual fear conditioning paradigm. Linear correlation plots between (**A**) context conditioned freezing or (**B**) mean extinction freezing versus regional delta FosB cell counts (ΔFosB+ cells) are shown. (**A**) Conditioned freezing showed a significant positive correlation with the central nucleus of the amygdala (CeA) ΔFosB+ cells and an inverse correlation with the dorsal dentate gyrus (dDG). (**B**) Mean extinction freezing showed a significant inverse linear correlation with ΔFosB+ cell counts in the infralimbic cortex (IL) and an inverse correlation with the dorsal dentate gyrus (dDG).

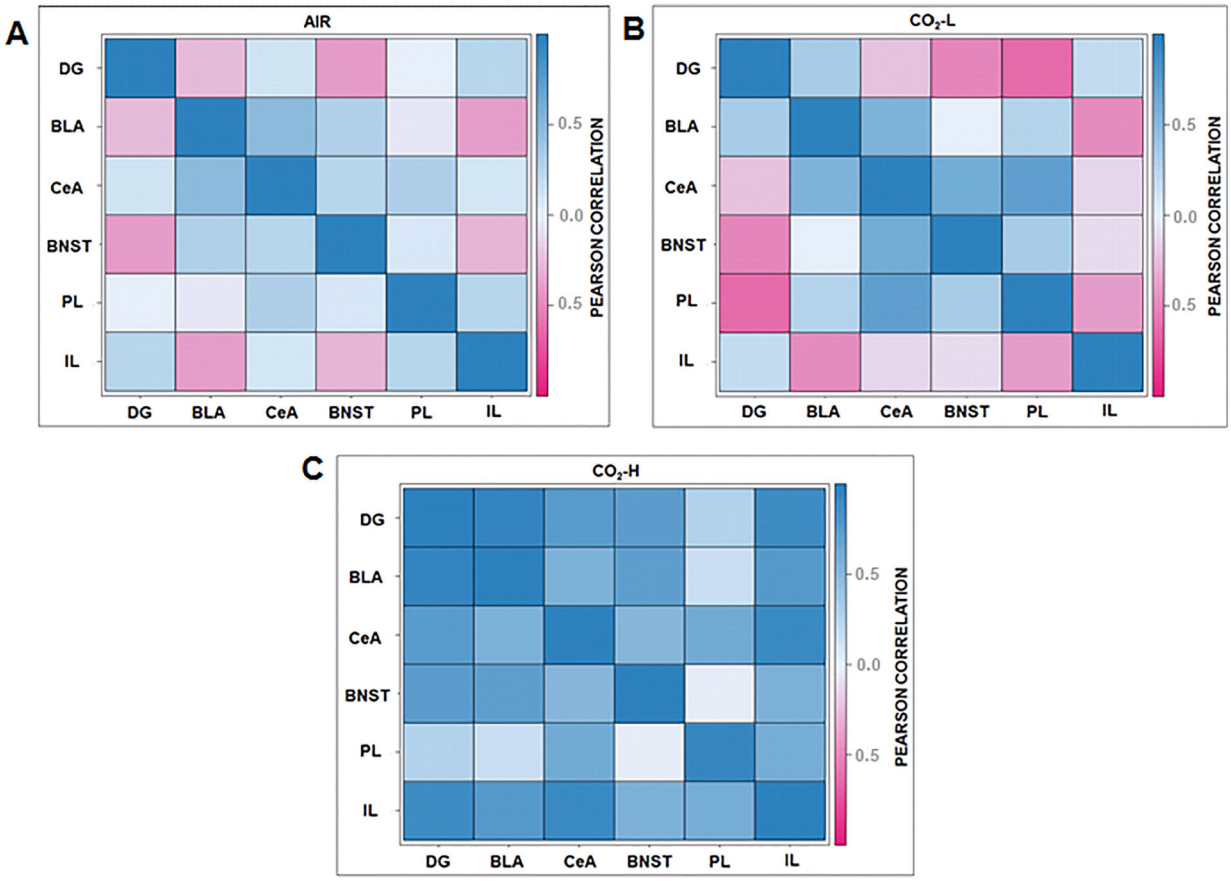

Fig. 7.

ΔFosB interregional correlation matrices reveal differential patterns of co-activation between (**A**) air, (**B**) CO_2-L and (**C**) CO_2-H. Co-activation patterns of forebrain areas such as the dDG and IL with the CeA, BLA, PL and BNST observed in air and CO_2-L mice were disrupted in CO_2-H mice. Positive dDG-amygdala and dDG-BNST co-activation patterns that were not observed in the other groups. An inverse co-activation association between IL-PL and IL-BLA was observed in CO_2-L mice that was absent in CO_2-H group. Dark blue represents strong positive correlations while dark pink represents strong negative correlations. Abbreviations: dDG, dorsal dentate gyrus; BLA, basolateral amygdala, CeA, central nucleus of the amygdala, IL, infralimbic cortex; PL, prelimbic cortex; BNST, bed nucleus of stria terminalis. (N = 6–8/group).

Table 1.

Association of air or CO_2 inhalation with startle reactivity and contextual fear conditioning-extinction. Compilation of Spearman correlations (*r*) between freezing to air (upper panel) or CO2 inhalation (lower panel) with startle amplitude and freezing during different phases of the fear conditioning paradigm

	Startle-0 db	**Startle-95 db**	**Startle-100 db**	**Startle-110 db**	**Startle-115 db**	**Startle-120 db**	**FC-hab**	**FC-Shock1**	**FC-Shock2**	**FC-Shock3**	**FC-CF**	**FC-E1**	**FC-E2**	**FC-E3**	**FC-E4**	**FC-E5**	**FC-Reinstatement**
Air																	
Number of *XY* Pairs	19	19	19	19	19	19	20	20	20	20	20	20	20	20	20	20	20
Spearman *r*	−0.2758	−0.1842	0.0422	0.1035	−0.0175	−0.0070	0.3392	0.0855	0.1188	−0.1113	−0.0060	0.2481	0.0369	0.2557	0.1699	0.2948	0.0015
95% confidence interval	−0.6571 to 0.2179	−0.5986 to 0.3079	−0.4321 to 0.4981	−0.3806 to 0.5431	−0.4794 to 0.4519	−0.4712 to 0.4602	−0.1355 to 0.6873	−0.3832 to 0.5192	−0.3541 to 0.5434	−0.5380 to 0.3608	−0.4586 to 0.4491	−0.2318 to 0.6309	−0.4241 to 0.4826	−0.2241 to 0.6358	−0.3076 to 0.5791	−0.1836 to 0.6603	−0.4527 to 0.4550
P value (two-tailed)	0.253	0.450	0.864	0.673	0.943	0.977	0.143	0.720	0.618	0.641	0.980	0.292	0.877	0.277	0.474	0.207	0.995
P value summary	ns	ns	ns	ns	ns	ns	ns	ns	ns	ns	ns	ns	ns	ns	ns	ns	ns
CO 2																	
Number of *XY* Pairs	18	18	18	18	18	18	19	19	19	19	19	19	19	19	19	19	19
Spearman *r*	−0.1748	0.3087	0.5831	0.4551	0.1755	0.4076	0.6082	0.3726	−0.1290	−0.0176	0.2789	0.1702	0.5509	0.5140	0.4158	0.2175	0.1035
95% confidence interval	−0.6029 to 0.3316	−0.1993 to 0.6860	0.1449–0.8300	−0.03002 to 0.7667	−0.3309 to 0.6034	−0.08815 to 0.7416	0.1987–0.8369	−0.1127 to 0.7144	−0.5610 to 0.3582	−0.4794 to 0.4519	−0.2147 to 0.6591	−0.3210 to 0.5892	0.1145–0.8090	0.06351–0.7905	−0.06193 to 0.7385	−0.2762 to 0.6204	−0.3806 to 0.5431
P value (two-tailed)	0.488	0.213	0.011	0.058	0.486	0.093	0.006	0.116	0.599	0.943	0.248	0.486	0.015	0.024	0.077	0.371	0.673
P value summary	ns	ns	*	#	ns	#	*	ns	ns	ns	ns	ns	*	*	#	ns	ns

* $p<0.05$,

\# $p=0.058$ (startle 110 db), $p=0.093$ (startle 120 db) $p=0.077$ (extinction D4).

Table 2.

Freezing during conditioned fear (upper panel) and mean extinction freezing (lower panel) was correlated with delta FosB cell counts in forebrain regions. Note positive correlation of freezing with amygdala subdivisions and negative correlations with infralimbic (IL) cortex and hippocampal dentate gyrus (DG)

	Fos-BLA	**Fos-CeA**	**Fos-DG**	**Fos-IL**	**Fos-PL**	**Fos-BNST**	**Fos-NAc**
Freezing (Conditioned Fear)							
Number of *XY* Pairs	23	23	23	23	20	22	22
Pearson/Spearman *r*	0.4003	0.5451	−0.4191	−0.3533	0.2492	−0.03004	−0.3033
95% confidence interval	−0.02732 to 0.7041	0.1587–0.7867	−0.7153 to 0.004759	−0.6754 to 0.08188	−0.2174 to 0.6231	−0.4461 to 0.3967	−0.6428 to 0.1358
P value (two-tailed)	0.0584	0.0071	0.0465	0.0981	0.2893	0.8944	0.1701
P value summary	#	*	*	#	ns	ns	ns
Pearson (normal) or Spearman (Gaussian Approx)	Spearman	Spearman	Spearman	Spearman	Pearson	Pearson	Pearson
Freezing (Extinction Mean)							
Number of *XY* Pairs	23	23	23	23	20	22	22
Pearson/Spearman *r*	0.06621	0.3221	−0.4733	−0.5237	0.2317	−0.135	−0.248
95% confidence interval	−0.3671 to 0.4759	−0.1168 to 0.6558	−0.7468 to −0.06293	−0.7750 to −0.1294	−0.2483 to 0.6203	−0.5362 to 0.3160	−0.6146 to 0.2068
P value (two-tailed)	0.7641	0.1339	0.0225	0.0103	0.3257	0.5492	0.2659
P value summary	ns	ns	*	*	ns	ns	ns
Pearson (normal) or Spearman (Gaussian Approx)	Spearman	Spearman	Spearman	Spearman	Pearson	Pearson	Pearson

* $p < 0.05$,

$p = 0.058$ (BLA), $p = 0.098$ (IL).